

A THRESHOLD THEOREM FOR THE RADIUS OF  
THE  $F_{2\nu}$  NUCLEON FORM FACTOR

Jeffrey Paul Royer

Stanford Linear Accelerator Center  
Stanford University, Stanford, California 94305

ABSTRACT

We developed a method for expanding the absorptive part of the sidewise dispersion relation for the nucleon  $F_{2\nu}$  radius. We assume that a threshold expansion is valid and we are able to obtain the exact first order terms in this expansion in the limit of the pion mass going to zero.

We are able to prove that the first order terms in this expansion come solely from the  $\pi$ -N intermediate state. Thus, the expansion provides justification for the retention of only the  $\pi$ -N intermediate state in a first attempt at describing the radius, as in Drell and Silverman.

Furthermore, the expansion provides a handhold for attempting to estimate the corrections to the first order term coming from the  $2\pi$ -N and higher intermediate states.

It must be emphasized that we are not providing justification for the assumption of threshold dominance. We are trying to follow that assumption to its logical conclusion. That is, if the threshold dominance idea is good, then a threshold expansion provides a logical way to calculate low-energy parameters. We have provided such an expansion for the  $F_{2\nu}$  radius.

\*Work supported by the U. S. Atomic Energy Commission.

(Submitted to Phys. Rev.)

# A THRESHOLD THEOREM FOR RADIUS OF THE $F_{2\nu}$ NUCLEON FORM FACTOR

## A. Introduction

In this paper we develop a method for expanding the absorptive part of the sidewise dispersion relation<sup>1</sup> for the nucleon  $F_{2\nu}$  radius. We assume that a threshold expansion is valid and we are able to obtain the exact first order terms in this expansion, in the limit of the pion mass going to zero.

We are able to prove that the first order terms in this expansion come solely from the  $\pi$ -N intermediate state. Thus the expansion provides justification for the retention of only the  $\pi$ -N intermediate state in a first attempt at describing the radius as in Drell and Silverman.<sup>2</sup>

Furthermore, the expansion provides a handhold for attempting to estimate the corrections to the first order term coming from the  $2\pi$ -N and higher intermediate states.

We now repeat the proceeding in a more mathematical way.

The sidewise dispersion relation<sup>1</sup> for the  $F_{2\nu}$  nucleon form factor is

$$F_{2\nu}(l^2, M^2) = \frac{1}{\pi} \int_{(M+\mu)^2}^{\infty} \frac{d(W^2) \text{ABS } F_{2\nu}(l^2, W^2)}{W^2 - M^2}, \quad (1)$$

where  $M$  is the nucleon mass,  $\mu$  is the pion mass, and  $l$  is the 4-momentum of the electromagnetic current.

The radius<sup>3</sup> is the slope at  $l^2=0$ , so the dispersion relation for the radius is

$$F'_{2\nu}(0, M^2) = \frac{1}{\pi} \int_{(M+\mu)^2}^{\infty} \frac{d(W^2) \text{ABS } F'_{2\nu}(0, W^2)}{W^2 - M^2}, \quad (2)$$

where the prime denotes differentiation with respect to  $l^2$ .

In the limit of  $\mu \rightarrow 0$ , we expand  $\text{ABS } F'_{2\nu}(0, W^2)$  in powers of  $\frac{W^2 - M^2}{M^2}$ .

$$\text{ABS } F'_{2\nu}(0, W^2) = \sum_{n=0}^{\infty} C_n \left( \frac{W^2 - M^2}{M^2} \right)^n \quad (3)$$

We show that  $C_0, C_1, C_2$ , vanish and we find  $C_3$  is given entirely by the  $\pi$ -N intermediate state.

It must be emphasized that we are not providing justification for the assumption of threshold dominance. We are trying to follow that assumption to its logical conclusion. That is, if the threshold dominance idea is good, then a threshold expansion provides a logical way to calculate low-energy parameters. We have provided such an expansion for the  $F_{2\nu}$  radius.<sup>4</sup>

The method of expanding the absorptive part depends crucially on the limit  $\mu \rightarrow 0$ . The details of the expansion may be expressed simply as follows. We first find the leading terms in the absorptive part as  $\mu \rightarrow 0$ . We then expand these leading terms in powers of  $\frac{W^2 - M^2}{M^2}$ .

Drell and Silverman<sup>2</sup> provided a hint leading to the method of isolating the most important contribution as  $\mu \rightarrow 0$ . In their analysis, which retained only the  $\pi$ -N intermediate state (Fig. 1), it was observed that the dominant contribution as  $\mu \rightarrow 0$  comes from the pion-pole term of the time-reversed electroproduction amplitude. The explanation is simply that this term is most singular in the pion mass. The algebraic reason is seen as follows. The pion propagator in Fig. 2 carries the 4-momentum  $l$  of the electromagnetic current. When we differentiate with respect to  $l^2$  to find the radius, we must differentiate the propagator, which gives us a term more singular in the pion mass than any of the other terms,

$$\frac{d}{dl^2} \left[ \frac{1}{(q-l)^2 - \mu^2} \right]_{l^2=0} = \frac{-1}{\mu^4}, \text{ at threshold.} \quad (4)$$

Thus, the obvious question arises: Can we use an argument based on this observation to pick out the leading terms, as  $\mu \rightarrow 0$ , in the contribution to the absorptive part from higher mass intermediate states? We are able to answer this question in the affirmative by using PCAC and current algebra to isolate, at threshold, the pion pole terms which carry the 4-momentum  $l$  of the electromagnetic current. These terms give the most singular contribution to the absorptive part of the radius as  $\mu \rightarrow 0$ . In this manner, we isolate the dominant terms at threshold as  $\mu \rightarrow 0$ . We then expand these terms in  $\frac{W^2 - M^2}{M^2}$  to obtain the announced expansion.

In Part I. B, we undertake the explanation of the graphical methods employed to handle the multi-pion, nucleon intermediate state.

In Part I. C, we apply the graphical techniques to an analysis of the relevant matrix elements needed for the proof to the threshold theorem. C1 discusses the matrix element of the electromagnetic current and C2 discusses the matrix element of the nucleon source. We complete the proof of the theorem in Part I. D. Concluding remarks are contained in Part I. E.

## B. Development of Graphical Procedures

This section undertakes the explanation of the graphical methods employed in the discussion of the multi-pion, nucleon intermediate state. The graphs function as numonics for complicated analytical expressions much the same way as Feynman graphs function in Q. E. D. We use the graphs first to avoid cumbersome analytic expressions and second, to help the reader develop an intuition for the manner in which we handle the multi-pion, nucleon intermediate state. The graphs we define are essentially identical to those defined in Abarbanel and Nussinov.<sup>5</sup>

The basic object which we want to represent graphically is the Fourier transform of the matrix element of the time-ordered product of a given set of operators. For example,

$$\iint d^4x_1 d^4x_2 e^{-iq_1 \cdot x_1} e^{-iq_2 \cdot x_2} \langle f | T Q_1(x_1) Q_2(x_2) | i \rangle \quad (5)$$

is such an object.

$|i\rangle$  is some initial state

$|f\rangle$  is some final state

$Q_i(x_i)$  is some local operator carrying momentum  $q_i$

The graphical representation of this object would be that shown in Fig. 3. The two heavy lines are the initial and final states and the two wavy lines are the operators  $Q_1(x_1)$  and  $Q_2(x_2)$ . The blob represents our ignorance of what is going on in the interaction.

Our discussion will contain four different kinds of operators.

$$A_\alpha^\mu(x) \text{----- The non-strangeness changing, strong-interaction axial vector current.} \quad (6)$$

$$D_\alpha \equiv \partial_\mu A_\alpha^\mu(x) \text{-- The divergence of 6.} \quad (7)$$

$$V_\alpha^\mu(x) \text{----- The non-strangeness changing, strong-interaction vector current.} \quad (8)$$

$$J_{EM}^\mu(x) \text{----- The strong-interaction electromagnetic current.} \quad (9)$$

The graphical elements for these operators are shown in Table I. It will be clear from the graph whether  $V_\alpha^\mu(x)$  or  $J_{EM}^\mu(x)$  should be associated with the solid line.

Some operators will arise by using the following SU(2) current commutation relations.

$$\delta(x_{10}-x_{20}) \left[ A_{\alpha_1}^0(x_1), A_{\alpha_2}^{\mu_2}(x_2) \right] = i \epsilon_{\alpha_1 \alpha_2 \alpha_3} V_{\alpha_3}^{\mu_2}(x_2) \delta^4(x_1-x_2) \quad (10)$$

$$\delta(x_{10}-x_{20}) \left[ A_{\alpha_1}^0(x_1), V_{\alpha_2}^{\mu_2}(x_2) \right] = i \epsilon_{\alpha_1 \alpha_2 \alpha_3} A_{\alpha_3}^{\mu_2}(x_2) \delta^4(x_1-x_2) \quad (11)$$

$$\delta(x_{10}-x_{20}) \left[ A_{\alpha_1}^0(x_1), J_{EM}^{\mu_2}(x_2) \right] = i \epsilon_{\alpha_1 \alpha_2 \alpha_3} A_{\alpha_3}^{\mu_2}(x_2) \delta^4(x_1-x_2) \quad (12)$$

To represent this graphically we define the elements in Table II. The lower-most leg will enter the blob. Again, it will be clear from the graph whether the solid line is  $V_{\alpha}^{\mu}(x)$  or  $J_{EM}^{\mu}(x)$ .

Many soft-pion techniques take advantage of PCAC to relate the pion field to the divergence of the non-strangeness changing, axial vector current; that is through

$$\partial_{\mu} A_{\alpha}^{\mu}(x) = \mu^2 f_{\pi} \phi_{\alpha}(x) \quad (13)$$

where  $\phi_{\alpha}(x)$  is the pion interpolating field and  $f_{\pi}$  is the pion decay constant. The derivative is then removed from the time-ordered product and the resulting expression is examined in various low energy limits.

We will depend strongly on the graphical techniques to expand the matrix elements of products of  $D_{\alpha}$ 's; that is, we will give a graphical algorithm for pulling the derivatives out of the time-ordered product. We will find that by pulling the derivatives off of the  $D_{\alpha}$ 's, we expand our original graph into a set of graphs, each of which is a simple arrangement of chains of axial and vector currents.

To make the preceding statement clear, we next illustrate the use of the graphs in expanding the matrix elements of the  $D_{\alpha}$ 's. We will expand the following

expression,

$$\iint d\vec{x}_1 d\vec{x}_2 e^{-iq_1 \cdot x_1} e^{-iq_2 \cdot x_2} \langle f | T \partial_\mu A^\mu_{\alpha_1}(x_1) \partial_\nu A^\nu_{\alpha_2}(x_2) | i \rangle \quad (14)$$

which is represented graphically in Fig. 4. The first step is to take the derivative of the first operator outside of the time-ordered product. When this is done, we obtain two terms. One term is just the derivative acting on the whole matrix element and the other term is an equal-time commutator coming from the action of the derivative on the theta function of the time-ordered product. Explicitly, expression (14) equals

$$\begin{aligned} & \iint d\vec{x}_1 d\vec{x}_2 e^{-iq_1 \cdot x_1} e^{-iq_2 \cdot x_2} \partial_\mu \langle f | A^\mu_{\alpha_1}(x_1) \partial_\nu A^\nu_{\alpha_2}(x_2) | i \rangle \\ & - \iint d\vec{x}_1 d\vec{x}_2 e^{-iq_1 \cdot x_1} e^{-iq_2 \cdot x_2} \delta(x_{10} - x_{20}) \langle f | [A^0_{\alpha_1}(x_1), \partial_\nu A^\nu_{\alpha_2}(x_2)] | i \rangle \end{aligned} \quad (15)$$

It would serve us well at this point to remark that we will neglect all commutators of the type arising in the second part of expression (15). This commutator is the well-known "sigma" term. We neglect this term because  $\partial_\mu A^\mu \propto \mu^2$  and we will ultimately be interested in the limit  $\mu \rightarrow 0$ . As long as there is no pion pole in the  $\sigma$  field, this  $\sigma$ -term will go to zero faster than the singular terms which we show to exist in this limit. So, neglecting the  $\sigma$ -term, we are left with just the first term in expression (15). We now perform an integration by parts, changing the derivative to a momentum. This is justified as long as the matrix elements of the operators do not grow as  $x, t \rightarrow \infty$ . The result then is that

$$\begin{aligned} & \iint d\vec{x}_1 d\vec{x}_2 e^{-iq_1 \cdot x_1} e^{-iq_2 \cdot x_2} \langle f | T \partial_\mu A^\mu_{\alpha_1}(x_1) \partial_\nu A^\nu_{\alpha_2}(x_2) | i \rangle \\ & = iq_{1\mu} \iint d\vec{x}_1 d\vec{x}_2 e^{-iq_1 \cdot x_1} e^{-iq_2 \cdot x_2} \langle f | T A^\mu_{\alpha_1}(x_1) \partial_\nu A^\nu_{\alpha_2}(x_2) | i \rangle \end{aligned} \quad (16)$$

The graphs which correspond to Eq. (16) is shown in Fig. 5. We see two conventions implicit in Fig. 5.

1. We will assume all currents flow into the blob.
2. An axial current connected to a blob is assumed to be dotted with  $iq_\mu$ , its momentum.

We now proceed in the same manner to remove the derivative from the second current. This time however, the equal-time commutator is non-negligible. Using the commutation relation (10), we obtain the following expression

$$\begin{aligned}
 & \iint d\vec{x}_1 d\vec{x}_2 e^{-iq_1 \cdot x_1} e^{-iq_2 \cdot x_2} \langle f | T \partial_\mu A^\mu_{\alpha_1}(x_1) \partial_\nu A^\nu_{\alpha_2}(x_2) | i \rangle \\
 &= iq_{1\mu} iq_{2\nu} \iint d\vec{x}_1 d\vec{x}_2 e^{-iq_1 \cdot x_1} e^{-iq_2 \cdot x_2} \langle f | T A^\mu_{\alpha_1}(x_1) A^\nu_{\alpha_2}(x_2) | i \rangle \\
 & \quad - iq_{1\mu} i \epsilon_{\alpha_2 \alpha_1 \alpha_3} \int d\vec{x}_2 e^{-i(q_1 + q_2) \cdot x_2} \langle f | V^\mu_{\alpha_3}(x_2) | i \rangle
 \end{aligned} \tag{17}$$

Equation (17) is represented graphically in Fig. 6. We note the following conventions.

1. There is a negative sign for each equal-time commutator.
2. The indices on the anti-symmetric epsilon are represented clockwise on the graph.
3. The solid line is  $V^\mu_\alpha(x)$ , not  $J^\mu_{EM}(x)$ .  $J^\mu_{EM}(x)$  can only appear when it is in the matrix element to begin with.

What we need to know is how to get the graphs without writing the analytic expressions. This is done by simply changing the symbol for the divergence into an axial and adding the symbols for the various equal-time commutators which arise from the other operators in the matrix element. To insure correct ordering of the  $\epsilon_{ijk}$  symbols, we make the convention that we attach the symbol representing  $A^0_\alpha(x)$  into the left side of the other two operators in the vertex.



We now work out a second example to illustrate the graphical method.

Figure 7 shows a step-by-step reduction of a graph into a sum of graphs by the method stated above. In Fig. 7, we leave off the lines representing the initial and final states to simplify the graphs.

The analytic expression for this reduction is

$$\begin{aligned}
& \iint d\vec{x}_1 d\vec{x}_2 e^{-iq_1 \cdot x_1} e^{-iq_2 \cdot x_2} \langle f | T \partial_{\mu_1} A_{\alpha_1}^{\mu_1}(x_1) \partial_{\mu_2} A_{\alpha_2}^{\mu_2}(x_2) J_{EM}^{\mu}(0) | i \rangle \\
&= iq_{1\mu_1} iq_{2\mu_2} \iint d\vec{x}_1 d\vec{x}_2 e^{-iq_1 \cdot x_1} e^{-iq_2 \cdot x_2} \langle f | T A_{\alpha_1}^{\mu_1}(x_1) A_{\alpha_2}^{\mu_2}(x_2) J_{EM}^{\mu}(0) | i \rangle \\
&\quad - iq_{1\mu_1} i\epsilon_{\alpha_2 \alpha_1 \alpha_3} \int d\vec{x}_1 e^{-i(q_1+q_2) \cdot x_1} \langle f | T V_{\alpha_3}^{\mu_1}(x_1) J_{EM}^{\mu}(0) | i \rangle \\
&\quad - iq_{2\mu_2} i\epsilon_{\alpha_1 \alpha_2 \alpha_3} \int d\vec{x}_2 e^{-iq_2 \cdot x_2} \langle f | T A_{\alpha_2}^{\mu_2}(x_2) A_{\alpha_3}^{\mu}(0) | i \rangle \\
&\quad - iq_{1\mu_1} i\epsilon_{\alpha_2 \alpha_3 \alpha_1} \int d\vec{x}_1 e^{-iq_1 \cdot x_1} \langle f | T A_{\alpha_1}^{\mu_1}(x_1) A_{\alpha_3}^{\mu}(0) | i \rangle \\
&\quad + i\epsilon_{\alpha_1 \alpha_3 \alpha_2} i\epsilon_{\alpha_2 \alpha_3 \alpha_4} \langle f | V_{\alpha_4}^{\mu}(0) | i \rangle
\end{aligned} \tag{18}$$

There are two more things to be mentioned before leaving this section. Since we are going to be dealing with pions, via PCAC, we will want the amplitude to be symmetrized in the pion indices. This allows us to drop the current labels in the graphs. We now just write out the expression for a particular graph, assuming some convention for the current labels, then we symmetrize the expression and multiply it by the number of times that graph was repeated in the reduction. The set of graphs in Fig. 7 would then be shown as in Fig. 8.

Finally, we remove the explicit pion poles from the single axial currents by defining a new operator, which has no pion poles, via the relation,<sup>6</sup>

$$A_{\alpha}^{\mu} \equiv A'_{\alpha}{}^{\mu} - i q^{\mu} / \mu^2 \partial_{\nu} A'_{\alpha}{}^{\nu} \quad (19)$$

By using this relation, we can eliminate the type of graph where  $A^{\mu}$  enters the blob and replace it by  $A'^{\mu}$ . In doing so, it is found that the matrix element containing the divergence of the eliminated axial current is multiplied by the factor  $(1 - q^2 / \mu^2)$ . That is, the graphs of Fig. 8 would be changed to those of Fig. 9. The prime on the wiggly indicates  $A'$ . The result of the replacement is to add a prime to all single wiggly lines and to multiply the divergences by  $(1 - q_i^2 / \mu^2)$ , where  $q_i$  is the momentum of the respective divergence.

We can now use the reduction formula and PCAC to relate the divergences to pion in-states. The rules for writing out the graphs are summarized as follows:

1. Successively change each divergence to an axial plus commutators.
2. Put primes on all single wiggly lines and put factors of  $(1 - q_i^2 / \mu^2)$  for each divergence.
3. Put a factor  $(-1)^n$  on each graph where  $n$  is the number of vertices in the graph.
4. Put factors of  $i q^{\mu}$  on the axials which have not been used to commute something.
5. Symmetrize in the isospin indices.

A short cut to step one is to just list the different ways of combining the currents into chains and then multiply each possibility by its repetition number  $R$ .

$$R = \frac{\binom{N}{C_1} \binom{N-C_1}{C_2} \binom{N-C_1-C_2}{C_3} \dots}{R_1 \times R_2 \times R_3 \dots} \quad (20)$$

where

$N$  = total number of original axials in matrix element

$C_i$  = number of axials in chain of type  $i$

$R_i$  = number of chains of type  $i$ .

### C. Analysis of the Absorptive Part

Now we turn to the task of examining in detail the absorptive part of the  $F_{2\nu}$  form factor. We will use the graphical many soft-pion method to discover the dominant contributions to the absorptive part. The sense in which we use the word dominant was mentioned in the introduction and will be made explicit in the following. Roughly, we want to think of the absorptive part as being expanded simultaneously in the two parameters  $\frac{\mu^2}{M^2}$  and  $\frac{W^2 - M^2}{M^2}$ . It is in this way that we will obtain a threshold expansion for the absorptive part as  $\mu^2 \rightarrow 0$ .

The  $F_2$  nucleon form factor satisfies an un-subtracted sidewise dispersion relation.<sup>1</sup>

$$F_2(l^2, M^2) = \frac{1}{\pi} \int_{(M+\mu)^2}^{\infty} \frac{d(W^2)}{W^2 - M^2} \text{ABS } F_2(l^2, W^2) \quad (21)$$

$l^2$  is the invariant mass of the photon and  $W^2$  is the invariant mass of the off-mass-shell nucleon.

The absorptive part of the dispersion relation is given by<sup>7</sup>

$$\begin{aligned} \text{ABS } F_2(l^2, W^2) = & 1/2 \sum_{s=1}^2 \sqrt{\frac{p_0}{M}} \sum_n (2\pi)^4 \delta^4(p+1-p_n) \\ & \times \langle ps | J_{EM}^\mu(0) | n, p_n \rangle \langle n, p_n | \bar{\eta}(0) | 0 \rangle \nu_\mu^2(W^2) U(p, s) \end{aligned} \quad (22)$$

$\sum_n$  represents both the intermediate state sum and the corresponding phase space,  $\bar{\eta}(0) = \bar{\psi}(0)(\not{p} + \not{\gamma} - M)$  where  $\bar{\psi}(0)$  is a nucleon field operator, and  $\nu_\mu^2$  is a projection operator which projects out the  $F_2$  part. This expression for the absorptive part becomes clearer when we look at Fig. 10.

The absorptive part is given by the product of two matrix elements. We see the off-shell nucleon (solid line) enter a strong interaction blob and emerge into an intermediate state  $|n\rangle$ . The intermediate state then goes into another blob and turns into an off-shell photon and a nucleon. The total absorptive part is then given by summing over all possible intermediate states and projecting out the part belonging to  $F_2$ .

The lowest mass intermediate state which can contribute is that containing one pion and one nucleon. The next most important states are those obtained by adding more pions. Adding four pions brings us up to a threshold of  $\sim 1500$  MeV where resonances such as those in Table III, begin to make contributions to the absorptive part.

We remind the reader at this point that the object of this work is to follow the threshold dominance idea to its logical conclusion. If the threshold dominance idea is valid, then it should be best implemented by providing an expansion about the threshold. We provide a method for determining the coefficient of the leading term and for estimating the higher order terms of this expansion. If the numerical results obtained from this expansion are in wild disagreement with experiment, this would lead us to suspect that threshold dominance doesn't apply here and that contributions from resonances and higher intermediate states farther along the cut must be taken into account.

We will be working from the point of view that the resonant contributions are really enhancements of some many-pion, nucleon state and it is only the contribution

to the threshold expansion as  $\mu^2 \rightarrow 0$  which will interest us. Thus, we will be considering only states with one nucleon and  $n$  pions.

The first step toward the threshold expansion is to examine each of the matrix elements in the absorptive part. We do this by expanding the matrix element according to the graphical method in Part I. B. For example, we would apply the graphical expansion to the matrix elements represented in Fig. 11 for the one-pion, nucleon intermediate state and to those represented in Fig. 12 for the two-pion, nucleon intermediate state.

After we expand the matrix elements according to the graphical description, we will examine the graphs to determine which graphs give the most singular (in  $\mu^2$ ) contribution to the radius at threshold. We will then make a threshold expansion of those most singular graphs.

Through the graphical description we are able to deal with the case of  $n$  pions almost as easily as with the cases of one or two pions. This results from the fact that there are basically only four different types of chains which enter into the strong-interaction blob of the graphs. We can examine each of these in detail near threshold and actually determine their singularity structure as  $\mu^2 \rightarrow 0$ .

In the following two sub-sections we will work first with the matrix element of the electromagnetic current and second with the matrix element of the nucleon source. Before embarking on this however, we must remark that we are making an expansion in powers of  $\frac{W^2 - M^2}{M^2}$  and that we will set  $\mu^2 \rightarrow 0$  everywhere where it doesn't result in a singularity. In particular, this means that threshold is at  $M^2$  and that the  $q_{i\mu} \rightarrow 0$  as we approach threshold, (all four components). Therefore we will set  $q_{i\mu} = 0$  everywhere except in those graphs where the singularity occurs.

## 1. Electromagnetic current matrix element

In this section, we study the matrix elements of the electromagnetic current.

$$\langle ps | J_{EM}^\mu(0) | ks', q_1 \alpha_1 \dots q_n \alpha_n \rangle \quad (23)$$

We show that certain types of graphs dominate the graphical expansion as  $\mu^2 \rightarrow 0$ . Our search for the dominant graphs was strongly motivated by the clue given by Drell and Silverman.<sup>2</sup> This clue indicated that the strongest singularities would occur in those graphs which had an axial current carrying the electromagnetic momentum into the blob. That is, the dominant graphs would have a chain which started with the electromagnetic current and ended with an axial current connected to the blob, (see Fig. 13 for an example). We show explicitly that it is only the above type of chain which can lead to strong singularities in the pion mass at threshold.

Suppose we start with the matrix element shown in Fig. 14. When we perform the graphical expansion of the graph in Fig. 14, we obtain a sum of graphs, each of which is a blob with various chains attached, (see Part I. B on graphical expansion). The important fact to be noted is that there are only four different types of chains. These are classified as follows:

- A. Chain without the electromagnetic current, ending in a vector.
- B. Chain without the electromagnetic current, ending in an axial.
- C. Chain containing the electromagnetic current, ending in a vector.
- D. Chain containing the electromagnetic current, ending in an axial.

Examples of these four types of chains are shown in Fig. 15.

Every graph in the graphical expansion is just a blob with various combinations of the above types of chains attached. The chapter on graphical expansion explains the details of the expansion. We need be concerned only as far as knowing what the general term looks like. Each blob will contain one chain of either type C or D. The remainder of the chains will be made of combinations of types A and B.

What we propose to do is to examine the behavior of the above chains as we near threshold to see whether singularities in the pion mass occur. We first consider chains of type A. We suppose that a chain of type A is attached to a blob along with other unspecified types of chains, (see Fig. 16).

The analytic expression for such a blob can be written as,

$$A = q_{j\mu} \int d^4x dR e^{-i\sum q_i \cdot x} \langle ps | TA_\alpha^\mu(x) \hat{O} | ks' \rangle \quad (24)$$

where the  $q_{i\mu}$  are the momentums of the axials connected to the chain,  $q_{j\mu}$  is the momentum of the axial which hasn't commuted anything,  $\hat{O}$  represents all other operators in the time-ordered product, and the  $dR$  represents all other exponential factors and space-time integrals for the operators in  $\hat{O}$ . We have omitted the  $\epsilon_{ijk}$  symbols and factors which are not essential to our argument.

We want to examine this expression when  $\mu^2 \rightarrow 0$  nears the threshold, which means that all four components of  $q_{i\mu} \rightarrow 0$ . In this case the entire expression vanishes except for contributions from nucleon pole terms.

The contribution from the pole term in the  $q_{i\mu} \rightarrow 0$  limit is that calculated by attaching the chain to the external nucleon leg,<sup>8</sup> (see Fig. 17). In this limit:

$$A = iq_{1\mu} \int dR \frac{\bar{U}(p, s) \left[ \gamma^\mu \gamma_5 g_A \tau_\alpha [\not{p} + M] \hat{O}' \right]}{-2p \cdot \sum q_i} \quad (25)$$

$$+ iq_{1\mu} \int dR \frac{\hat{O}' (k + M) \gamma^\mu \gamma_5 g_A \tau_\alpha U(k, s')}{2k \cdot \sum q_i}$$

where  $\hat{O}'$  is essentially the time-ordered product of the operators  $\hat{O}$ . We see from this that A is finite in this limit and that the chain of type A cannot lead to singularities in the pion mass. Any singularities must occur in  $\hat{O}'$ .

The analysis of chains of type B proceeds similarly to the analysis of chains of type A, with the exception that the form factors are changed from axial form factors to vector form factors, and the  $\gamma_5$  is omitted;

$$B = q_{j\mu} \int d\mathbf{x}^4 dR e^{-i\sum q_i \cdot x} \langle ps | TV_\alpha^\mu(x) \hat{O} | ks' \rangle \quad (26)$$

with the same conventions as before. In the limit  $\mu^2 = 0$ ,  $q_{i\mu} \rightarrow 0$ , B becomes

$$B = iq_{j\mu} \int dR \frac{\bar{U}(p, s) (\gamma^\mu F_1 \tau_\alpha) (\not{p} + M) \hat{O}'}{-2p \cdot \sum q_i} \quad (27)$$

$$+ iq_{j\mu} \int dR \frac{\hat{O}(k + M) \gamma^\mu F_1 \tau_\alpha U(k, s')}{2k \cdot \sum q_i}$$

Again, as in A, this is finite as  $q_{i\mu} \rightarrow 0$  and the only place singularities can occur is in  $\hat{O}'$ . The analysis of chains C and D differs slightly from that of A and B. We will assume that all of the chains of types A and B have already been analyzed before proceeding with the analysis of C and D. Since each chain of type A or B is attached to the external nucleon legs as we approach threshold, the result after the analyses of all A and B chains is that C or D is sandwiched directly between nucleons. This is shown symbolically in Fig. 18.

The contribution of a C or D type chain then comes down to its matrix element between nucleons. Type C gives the vector form factors of the nucleon and type D gives the axial vector form factors of the nucleon. It is easy to see that the type



C chain is non-singular as  $\mu^2 \rightarrow 0$  because there are no pion poles in the vector form factors.<sup>9</sup> There is however, a pion pole in the induced pseudo-scalar form factor which is of the type we would expect to be important from the clue in Drell and Silverman.<sup>2</sup> This pion pole will carry the momentum  $\sum q_i + 1$  where the  $q_i$  are the momenta entering the chain.

This will have the form

$$\propto \frac{1}{\mu^2 - (q_i + 1)^2} \xrightarrow{q_i \mu \rightarrow 0} \frac{1}{\mu^2 - 1^2} \quad (28)$$

which will give  $\frac{1}{\mu^4}$  when we differentiate to find the radius.

We have analyzed the matrix element of the electromagnetic current by analyzing separately each of the 4 possible types of chains which can be attached to the strong interaction blob coming from the graphical expansion. Of these chains, only that of type D, an axial current entering the blob and carrying the electromagnetic momentum 1, can contribute a singularity as  $\mu^2 \rightarrow 0$ . Since these can be only one chain of type D attached to any particular blob, the order of the singularity cannot be greater than  $\frac{1}{\mu^4}$ . The contributions from the chains A, B, and C are finite as  $\mu^2 \rightarrow 0$  at threshold and are easily calculated as discussed in the preceding. The upshot is that we will keep only those graphs in the expansion which contain chains of type D. In Fig. 19, we show the expansion of the 1, 2, and 3 pion cases in terms of graphs, and underline the dominant graphs.

As we approach the threshold in the  $\mu^2 = 0$  limit, the underlined graphs simplify further to the graphs shown in Fig. 20, where the A, B, C, and D type chains are attached as indicated from the preceding analysis.

We might mention at this point that if we considered a pure  $\mu^2 = 0$  theory, the radius would in fact be infinite due to the graphs which had a pion pole carrying the electromagnetic momentum.<sup>10</sup> That is, the underlined graphs above would behave

like  $\frac{1}{2}$  at threshold instead of  $\frac{1}{2-\mu}$ . Thus in a pure  $\mu^2 = 0$  theory, the underlined graphs would indeed dominate the others, in fact, the finiteness of the other graphs would make them negligible compared to those underlined. When we give the pion a finite non-zero mass, we are increasing the importance of the neglected graphs compared to those underlined. This importance is measured then by the size of the pion mass relative to the nucleon mass, which is the expansion parameter in this problem.

## 2. Matrix element of the nucleon source

Now, we turn to the matrix element of the nucleon source.

$$\langle ks', q_1 \alpha_1, \dots, q_n \alpha_n | \bar{\eta}(0) | 0 \rangle \quad (29)$$

Our first concern is to determine whether or not this matrix element can be singular in the pion mass as we near threshold. If we attempt to apply the graphical analysis of the previous sections to the above matrix element, the following unknown commutator arises.

$$\delta(x_0 - y_0) \left[ A_\alpha^0(x), \bar{\psi}(y) \right] \quad (30)$$

If we assume that this commutator vanishes outside the light-cone so as to be consistent with microscopic causality, then Eq. (30) must be proportional to a 4-dimensional delta function or derivatives of such a delta function. It must also be proportional to a field which can create and destroy a nucleon. The simplest expression which has the correct transformation properties and is consistent with the above requirements is

$$\delta^4(x-y) \bar{\psi}(x) \gamma_5^\tau \alpha \quad (31)$$

We will use the following relation, as a model, although the analysis of Eq. (29) doesn't depend on this particular model. We choose this form for the sake of

convenience.

$$\delta(x_0 - y_0) \left[ A_\alpha^0(x), \bar{\psi}(y) \right] = \delta^4(x-y) \bar{\psi}(x) \gamma_5 \tau_\alpha \quad (32)$$

We could replace the  $\bar{\psi}(x)$  on the right by some arbitrary function which transforms like  $\bar{\psi}(x)$  and which can create and destroy a nucleon. We could also add terms which are proportional to derivatives of  $\delta^4(x-y)$ . None of these changes in themselves could make the matrix element singular as  $\mu^2 \rightarrow 0$ . The key assumption we have made is that the matrix element of the commutator itself does not blow up in the  $\mu^2 = 0$  limit.

This assumption is very reasonable in view of the fact that the terms which arise because of the above equal-time commutators only contribute additions to the on-shell matrix element, proportional to some power of  $\frac{W^2 - M^2}{M^2}$ . This fact follows by setting the off-shell invariant mass equal to  $M^2$ , and using the reduction formula to get rid of the nucleon field operator by changing it to a nucleon in-state. The absence of the field operator prevents any terms from arising in the graphical reduction which contain the above commutator. Thus, as the off-shell nucleon mass goes from  $W^2$  to  $M^2$ , the contributions from the graphs containing commutators vanish independently of the pion mass. Therefore, these terms can't be singular in the pion mass.

Now, if we apply the graphical techniques to Eq. (29), using the model (Eq. (32)), we will end up with a sum of graphs, each of which is of the general type shown in Fig. 21. That is, the matrix elements represented by the graphs will be the time-ordered product of a nucleon field with a number of chains of types A and B, sandwiched between a final nucleon  $|k, s\rangle$  and the vacuum.

We examine these chains exactly as we did the similar chains in the preceding section. The chains come out of the time-ordered product and are attached to the external nucleon leg. Their contribution is finite and non-singular as  $q_{i\mu} \rightarrow 0$  and

$\mu^2 \rightarrow 0$ . The matrix element left after the removal of all of the chain is the matrix element of the nucleon source connecting  $|ks\rangle$  to the vacuum. This final matrix element is just the wave function and does not have any pion poles. Therefore, there is no possibility here of a pion pole singularity and all we must be concerned with is the expansion of Eq. (29) in  $\frac{W^2 - M^2}{M^2}$ .

#### D. Completion of Proof

We have studied the two matrix elements and have determined the following program:

1. With regard to  $\langle ps | J_{EM}^\mu(0) | ks' q_1 \alpha_1 \dots q_n \alpha_n \rangle$ , we will keep only those graphs of the graphical expansion which are most singular in the pion mass, i. e., terms which contain a chain of type D. These singular graphs will be expanded in powers of  $\frac{W^2 - M^2}{M^2}$ .
2. With regard to  $\langle ks' q_1 \alpha_1 \dots q_n \alpha_n | \eta(0) | 0 \rangle$ , we have shown that we obtain no pion mass singularities, therefore, all we need to do is expand this in powers of  $\frac{W^2 - M^2}{M^2}$ .
3. We will evaluate the phase space integral at threshold, assuming the matrix elements to be constant at their threshold value. The threshold behavior of the phase space for 1 massive and n massless particles can be calculated<sup>11</sup> and the result is that the phase space behaves like  $\left(\frac{W^2 - M^2}{M^2}\right)^{2n-1}$ . This behavior of phase space is crucial in our final argument. We can count on an extra factor of  $\left(\frac{W^2 - M^2}{M^2}\right)^2$  for each additional pion.

By combining 1, 2, and 3 above, we can show that the leading contribution to the threshold expansion of the absorptive part of the radius comes from only the  $\pi$ -N intermediate state. This result is obtained by merely counting powers of the threshold expansion parameter.

For the intermediate state with one pion and a nucleon, the product of the matrix elements gives two powers of  $\frac{W^2 - M^2}{M^2}$ . This, multiplied by the appropriate phase space gives a total of three powers of  $\frac{W^2 - M^2}{M^2}$ .<sup>12</sup>

For the intermediate state with two pions and a nucleon, the product of the matrix elements gives at least one power of  $\frac{W^2 - M^2}{M^2}$ .<sup>13</sup> The phase space gives three powers which yields a total of four powers, or at least one more than the one pion, nucleon state gives.

The phase space with three pions is already five powers of  $\frac{W^2 - M^2}{M^2}$ , so we do not have to calculate the product of the matrix elements. This information is summarized in Table IV.

So we see this result; the lowest order term in the threshold expansion of the absorptive part of the radius of  $F_{2\nu}$ , in the  $\mu^2 \rightarrow 0$  limit, comes entirely from the  $\pi$ -N state.

#### E. Conclusion

The theorem proves that the  $\pi$ -N intermediate state is the major contributor in the calculation of the  $F_{2\nu}$  radius with the sidewise dispersion relation. This fact has been, of course, conjectured, assumed, hoped for, and used with success since the advent of the sidewise dispersion relation.<sup>14</sup> However, the words "major contributor" remained vague and unqualified, somehow meaning that we did need to consider the intermediate states containing more pions. The proof of this theorem now provides a precise statement of the meaning of the words "major contributor." This precise statement arises from the analysis of the contribution of the various intermediate states to the terms of an expansion in the parameter  $\frac{W^2 - M^2}{M^2}$  as  $\mu/M \rightarrow 0$ .

The utility of this statement is not completely clear because  $\mu/M \sim 1/7$ , which means that corrections of order 15% may come by just considering the

next terms in  $\mu/M$ . Also, we have no guarantee that the threshold expansion converges. As with most expansions in physics, we must calculate the expansion coefficients to determine whether or not the expansion is useful.

The results of Drell and Silverman<sup>2</sup> indicate that the threshold expansion for the  $F_{2V}$  radius does converge rapidly and that the  $\pi$ -N intermediate state gives most of the radius.

The question arises as to why we can't make a similar theorem for the calculation of the anomalous moment. We probably could produce such a theorem but results show that the contributions from the  $S_{11}$  and  $P_{11}$  resonances make significant contributions to the anomalous moment which means the threshold expansion would converge very slowly and would be of little utility.

We take the opportunity here to mention that we tried to use the formalism developed here to understand the large radii of the  $K_{13}$  form factors implied by the work of Probir Roy.<sup>15</sup> We failed to provide any dynamical reason for the large radii and we conclude that if it exists, it must be attributed to a subtraction constant.

## APPENDIX A

The on-shell vertex function,  $\Gamma_\mu(p, p+1)$ , is defined by

$$\langle p, s | J_{EM}^\mu(0) | p+1, s' \rangle \equiv \bar{U}(p, s) \Gamma^\mu(p, p+1) U(p+1, s') . \quad (33)$$

The reduction formula is used to analytically continue the vertex function in the (mass)<sup>2</sup> of the initial nucleon.<sup>1</sup> The most general form for the off-shell vertex, which transforms like a vector under proper Lorentz transformations and is restricted by the Dirac equation on the final spinor is<sup>16</sup>

$$\begin{aligned} \bar{U}(p, s) \Gamma_\mu(p, p+1) = \bar{U}(p, s) & \left\{ \left[ \gamma_\mu F_1^+(W^2, l^2) - \frac{i\sigma_{\mu\nu} l^\nu}{2M} F_2^+(W^2, l^2) \right. \right. \\ & \left. \left. + l_\mu F_3^+(W^2, l^2) \right] \times \frac{(\not{p} + \not{l} + M)}{2M} \right. \\ & \left. + \left[ \gamma_\mu F_1^-(W^2, l^2) - \frac{i\sigma_{\mu\nu} l^\nu}{2M} F_2^-(W^2, l^2) + l_\mu F_3^-(W^2, l^2) \right] \right. \\ & \left. \times \frac{(-\not{p} - \not{l} + M)}{2M} \right\} . \quad (34) \end{aligned}$$

The projection operators  $\nu_\mu^{i\pm}(W^2)$ , are defined as follows,

$$2M \sum_s \bar{U}(p, s) \Gamma^\mu(p, p+1) \nu_\mu^{i\pm}(W^2) U(p, s) = - F_i^\pm(W^2, l^2) \quad (35)$$

For the purposes of this paper, we need to know only  $\nu_\mu^{2+}(W^2)$ , which is derived in reference

$$\begin{aligned} \nu_\mu^{2+}(W^2) = \frac{(\not{p} + \not{l} + M)}{2M} & \left[ \gamma_\mu \alpha_1^{2+}(W^2) - \frac{i\sigma_{\mu\nu} l^\nu}{2M} \alpha_2^{2+}(W^2) + l_\mu \alpha_3^{2+}(W^2) \right] \\ & + \frac{(-\not{p} - \not{l} + M)}{2M} \left[ \gamma_\mu \beta_1^{2+}(W^2) - \frac{i\sigma_{\mu\nu} l^\nu}{2M} \beta_2^{2+}(W^2) + l_\mu \beta_3^{2+}(W^2) \right] \quad (36) \end{aligned}$$

$\alpha$  and  $\beta$  are given in Table V.

## APPENDIX B

In Appendix B, we discuss the contribution to the absorptive part from the one-pion, nucleon intermediate state. We show this contribution gives three powers of  $\frac{W^2 - M^2}{M^2}$  as stated in Part I. D above.

Using the graphical methods developed in Part I. B, we quickly work out the following expressions for the needed matrix elements. We start with the electromagnetic matrix element and use the reduction formula on the pion, plus PCAC, to obtain

$$\langle ps | J_{EM}^\mu(0) | ks', q\alpha \rangle = i/f_\pi \left( \frac{\mu^2 - q^2}{\mu^2} \right) \int \frac{d^4x e^{iq \cdot x}}{\sqrt{2q_0}} \langle ps | T J_{EM}^\mu(0) \partial_\nu A_\alpha^\nu(x) | ks' \rangle \quad (37)$$

Then we apply the graphical analysis to the right-hand side of Eq. (37), keeping only the pion-pole term, to obtain the following

$$\langle ps | J_{EM}^\mu(0) | ks', q\alpha \rangle = \frac{\epsilon_\alpha 3\beta}{\sqrt{2q_0} f_\pi} \langle ps | A_\beta^\mu(0) | ks' \rangle$$

or

$$= \epsilon_\alpha 3\beta \sqrt{\frac{M^2}{2q_0 E_p E_k}} \left( \frac{2Mg_A}{f_\pi} \right) \frac{(q-l)^\mu}{\mu^2 - (q-l)^2} \times \bar{U}(p, s) \gamma_5 \tau_\beta U(k, s') \quad (38)$$

We use the reduction formula in the following form to obtain an expression for the matrix element of the nucleon source, near threshold, i. e.,  $W^2 \rightarrow M^2$ .

$$-i(2\pi)^4 \delta^4(k+q-p-l) \langle ks', q\alpha | \bar{\eta}(0) | 0 \rangle = \sum_s \langle ks', q\alpha | p+1, s \rangle \bar{U}(p+1, s) \quad (39)$$

Using

$$\langle ks', q\alpha | p+1, s \rangle = i \int \frac{d^4x e^{iq \cdot x}}{\sqrt{2q_0}} \langle ks' | J_{\pi\alpha}(x) | p+1, s \rangle \quad (40)$$

we obtain

$$\langle ks', q\alpha | \bar{\eta}(0) | 0 \rangle = -ig_\pi \sqrt{\frac{M}{2q_0 E_k}} \bar{U}(k, s') \gamma_5 \tau_\alpha \quad (41)$$



Putting these two matrix elements in the expression for the absorptive part of  $F_2$ , we obtain

$$\begin{aligned}
 \text{ABS } F_{2I}^+(W^2, l^2) &= \frac{1}{2} \sqrt{\frac{E_p}{M}} \int \frac{d^3k d^3q (2\pi)^4 \delta^4(p+l-k-q)}{(2\pi)^6} \epsilon_{\alpha 3\beta} \sqrt{\frac{M^2}{2q_0 E_p E_k}} \left( \frac{2Mg_A}{f_\pi} \right) \\
 &\times \frac{(q-1)^\mu}{\mu^2 - (q-1)^2} \times (-ig_\pi) \sqrt{\frac{M}{2q_0 E_k}} \times \text{TR} \left[ \frac{(p+M)}{2M} \gamma_5 \frac{(k+M)}{2M} \gamma_5 \nu_{\mu}^{+2} \right] \\
 &\times \text{TR} \tau_{\beta}^{\tau} \alpha^{\tau} P_I \tag{42}
 \end{aligned}$$

The last trace is to project us onto either the isovector or isoscalar part. By doing the isospin trace, we see that there is no contribution to the isoscalar part in this order. To do the remaining trace we refer to Appendix A where the explicit forms of the projection operators are written out.

In doing the trace, we keep in mind that we are only concerned with finding out the order of the leading term. The calculation of these traces is straightforward but long and tedious.

We present the results of the traces in Table VI. Table VI contains six rows each labeled by an  $\alpha$  or a  $\beta$ . These  $\alpha$ 's and  $\beta$ 's correspond to those in the projection operator  $\nu_{\mu}^{2+}$  and thus label the contribution from those corresponding terms in the projection operator. The bracket labeled "angles" signifies a function which depends on the angles to be integrated over, but which is independent of  $\frac{W^2 - M^2}{M^2}$ .

The results in Table VI show that the first order contribution cancels and so the product of the matrix elements is of second order in  $\frac{W^2 - M^2}{M^2}$  as stated in Part I. D. The phase space integral gives us another power of  $\frac{M^2}{W^2 - M^2}$ . Thus the contribution to the absorptive part is of order three in  $\frac{W^2 - M^2}{M^2}$ .

## APPENDIX C

In Appendix C, we discuss the contribution to the absorptive part from the two pion, nucleon intermediate state. We show that this gives greater than or equal to four powers of  $\frac{W^2 - M^2}{M^2}$  as stated in Part I. D.

We will follow closely the analysis contained in Appendix B, leaving out some of the pedagogical in steps included there.

Using the graphs, we can immediately isolate the dominate parts of the electromagnetic current matrix element; i. e., those graphs which have a pion pole carrying the electromagnetic momentum. The result is,

$$\begin{aligned}
 \langle ps | J_{EM}^\mu(0) | ks', q_1 \alpha_1, q_2 \alpha_2 \rangle &= -i \epsilon_{\alpha_2 3 \beta} \left( \frac{2Mg_A^2}{f\pi} \right) \frac{(q_2 - 1)^\mu}{\mu^2 - (q_2 - 1)^2} \times \sqrt{\frac{M^2}{4q_1 q_2 E_p E_k}} \\
 &\times \bar{U}(p, s) \left[ \frac{\gamma_5 \tau_\beta (k + \not{q}_1 + M) \not{q}_1 \gamma_5 \tau_{\alpha_1}}{2k \cdot q_1} \right. \\
 &\left. + \frac{\not{q}_1 \gamma_5 \tau_{\alpha_1} (\not{p} - \not{q}_1 + M) \gamma_5 \tau_\beta}{-2p \cdot q_1} \right] U(k, s') \\
 &+ \text{terms with } 1 \leftrightarrow 2
 \end{aligned} \tag{43}$$

Similarly to the method in Appendix B, we obtain the following

$$\begin{aligned}
 \langle ks', q_1 \alpha_1, q_2 \alpha_2 | \bar{\eta}(0) | 0 \rangle &= \frac{-g_A^2}{f\pi} \sqrt{\frac{M^2}{4q_1 q_2 E_k}} \times \bar{U}(k, s') \left[ \frac{\tau_{\alpha_1} \not{q}_1 (k - M) \not{q}_2 \tau_{\alpha_2}}{2k \cdot q_1} \right] \\
 &+ i \epsilon_{\alpha_2 \alpha_1 \beta} \left( \frac{1}{4f\pi} \right) \sqrt{\frac{M^2}{4q_1 q_2 E_k}} \bar{U}(k, s') \not{q}_1 \tau_\beta \\
 &+ \text{terms with } 1 \leftrightarrow 2
 \end{aligned} \tag{44}$$

We will omit writing out the total expression for the absorptive part because it is long and cumbersome and it does not serve to elucidate anything. The isospin traces yield the same results as in the single pion case. There is no contribution to the isoscalar part of the  $F_2$  form factor in this order. The statement which was made in Part I.D requires that we obtain at least one power of  $\frac{W^2 - M^2}{M^2}$  from the product of the matrix elements. We can see that this is a fact in the following way. If we count powers of  $q_1$  in the traces to be done, we see that there is always one power. When we do the phase space integral at threshold, all the  $q_1$ 's are set to zero by the delta function, and the contribution to the absorptive part vanishes. As we move away from threshold  $W^2 \neq M^2$ , we can have a non-zero contribution but it must be proportional to at least the first power of  $\frac{W^2 - M^2}{M^2}$ .

The phase space for 1 massive and two massless particles gives three powers of  $\frac{W^2 - M^2}{M^2}$ . Combining these results, we get at least four powers of  $\frac{W^2 - M^2}{M^2}$  as stated.

## APPENDIX D

In Appendix D, we prove the following statement. The phase space for 1 massive and  $n$  massless particles goes like  $\left(\frac{W-M}{M}\right)^{2n-1}$  at threshold, where  $W$  is the total c. m. energy of the system. We follow the method of Stapp.<sup>17</sup>

We first make some definitions.

$$\prod_{i=1}^n \frac{d^3 k}{E_k} \frac{d^3 q_i}{E_i} = d^3 \bar{P} dE d\Omega d\Gamma \rho(\Omega, \Gamma, E)$$

$$\bar{P} = \bar{k} + \sum_{i=1}^n \bar{q}_i = \text{Total momentum in c. m. frame}$$

$$E = \text{Total c. m. energy} \quad (45)$$

The  $d\Omega$  and  $d\Gamma$  are defined as follows: First, make a Lorentz transformation to a frame where  $\bar{k}^1 + \bar{q}_1^1 = 0$ . The superscript indicates that we have made one Lorentz transformation.

Define  $\mathcal{M}_1 \equiv \sqrt{M^2 + k_{11}^2} + \sqrt{k_{11}^2} =$  energy of the massive particle and the first massless particle in their c. m. frame.

$$\bar{k}_{11} \equiv \bar{q}_1$$

Now, we make a second L. T. to a frame where  $\bar{k}^2 + \bar{q}_1^2 + \bar{q}_2^2 = 0$ , and define the c. m. energy of these three particles in the second frame.

$$\mathcal{M}_2 \equiv \sqrt{\mathcal{M}_1^2 + k_{22}^2} + \sqrt{k_{22}^2}, \quad \bar{k}_{22} \equiv \bar{q}_2 \quad (47)$$

Likewise, frame  $k$  is defined by  $\vec{k}^k + \sum_{i=1}^k \vec{q}_i^k = 0$ .

$$\mathcal{M}_k = \sqrt{\mathcal{M}_{k-1}^2 + k_{kk}^2} + \sqrt{k_{kk}^2}, \quad \vec{k}_{kk} = \vec{q}_k^k \quad (48)$$

$\mathcal{M}_n \equiv E$  = total e. m. energy of all particles.

Our new integration variables are

- i)  $d\vec{P}$  (3 variables)
- ii) angles of the  $\vec{k}_{ii}$  ( $2n$  variables)
- iii)  $d\mathcal{M}_i$  ( $n$  variables).

This is a total of  $3n + 3$  variables, or the correct number. We now define

$d\Omega \equiv$  angle differentials of the  $k_{ii}$

$$d\Gamma = \prod_{i=1}^n d\mathcal{M}_i$$

$\rho(\Omega, \Gamma, E)$  is worked out by finding the Jacobian of this transformation of variables.

$$\rho = \prod_{i=1}^n \frac{k_{ii}}{E}$$

The limits on the integrals over the  $\mathcal{M}$  are established by using the definition

$$\mathcal{M}_k > \mathcal{M}_{k-1} > M \quad (49)$$

So

$$\begin{aligned} \prod_{i=1}^n \int \frac{d^3 k_i}{E_k} \frac{d^3 q_i}{E_i} \delta^4(k + \sum_i q_i - Q) &= \int \frac{d^3 \vec{P} dE}{E} \delta^3(\vec{P}) \delta(E - W) \\ &\times \prod_{i=1}^n d\Omega_{ii} \int_M^E d\mathcal{M}_{n-1} \int_M^{\mathcal{M}_{n-1}} d\mathcal{M}_{n-2} \cdots \int_M^{\mathcal{M}_2} d\mathcal{M}_1 \prod_{i=1}^n k_{ii} \end{aligned} \quad (50)$$

In order to make the threshold dependence clear, we define new variables

$$n_i \equiv \frac{M_i - M_{i-1}}{E'}, \quad E' \equiv E - M$$

Then

$$\prod_{i=1}^n \int \frac{d^3 k}{E_k} \frac{d^3 q_i}{E_i} \delta^4(k + \sum_i q_i - Q) = \int \frac{d^3 \bar{P} dE}{E' + M} \delta^3(\bar{P}) \delta(E - W)$$

$$\times \prod_{i=1}^n d\Omega_{ii} \int_0^1 dn_1 \int_0^{1-n_1} dn_2 \dots \int_0^{1-\sum_{i=1}^{n-2} n_i} dn_{n-1} (E')^{n-1} \prod_{i=1}^n k_{ii}$$
(51)

We now need to see how  $\prod_{i=1}^n k_{ii}$  depends on  $E'$ .

Solving explicitly for  $k_{kk}$

$$k_{kk} = \frac{(E' n_k) \left( E' n_k + 2E' \sum_{i=1}^{k-1} n_i + 2M \right)}{2 \left( E' \sum_{i=1}^k n_i + M \right)}, \quad (52)$$

we see that each  $k_{kk}$  gives us an additional power of  $E'$ . When we count the total number of powers of  $E'$ , we get  $n-1$  powers from the differentials and  $n$  powers from the  $k_{kk}$ . The total is then  $(E')^{2n-1}$ . Since  $E' = W - M$ , we have  $\left( \frac{W - M}{M} \right)^{2n-1}$ .

Q. E. D.

## ACKNOWLEDGEMENTS

I would like to thank Dr. S. D. Drell for the initial suggestion of this problem and for his continuing guidance and encouragement during the resulting research.

## REFERENCES

1. A. M. Bincer, Phys. Rev. 118, 855 (1960).
2. S. D. Drell, and D. J. Silverman, Phys. Rev. Letters 20, 1325 (1968).
3. It is customary to define the form factor radius as follows:

$$\langle r^2 \rangle = \frac{6}{F(0)} \left. \frac{dF(l^2)}{dl^2} \right|_{l^2=0},$$

where  $l^2$  is the square of the electromagnetic 4-momentum and  $F$  is the form factor in question. For general definitions, see S. D. Drell and F. Zachariasen, Electromagnetic Structure of Nucleons, (Oxford University Press, Fair Lawn, New Jersey, 1961).

4. The reason we write  $F_{2V}$  is because:
  - (a) The sidewise dispersion relation for  $F_1$  contains a subtraction constant which may or may not be a function of  $l^2$ . Without knowledge of whether or not this is true, we cannot hope to calculate the radius of  $F_1$ . For a more extensive discussion of this, see D. J. Silverman, Ph.D. dissertation, Stanford University Physics Department, Stanford, California, (1968) (unpublished).
  - (b) We show explicitly in the appendix that the leading terms in the threshold expansion do not contribute to  $F_{2S}$ .
5. H. D. I. Abarbanel, and Shmuel Nussinov, Ann. of Phys. 42, 467 (1967).
6. The nucleon matrix element of  $A'$  can easily be calculated in terms of the usual pseudo-vector and induced pseudo-scalar form factors. Using the definition,

$$\langle p_2 | A'^{\mu}(x) | p_1 \rangle \equiv \langle p_2 | A^{\mu}(x) | p_1 \rangle + i q^{\mu} / \mu^2 \langle p_2 | \partial_{\nu} A^{\nu}(x) | p_1 \rangle$$



where  $q = p_2 - p_1$ , we obtain

$$\langle p_2 | A^\mu(0) | p_1 \rangle = \bar{U}(p_2) \{ g_A(q^2) \gamma^\mu \gamma_5 + q^\mu / \mu^2 [ h_A(q^2) (\mu^2 - q^2) - 2M g_A(q^2) ] \gamma_5 \} U(p_1).$$

If we use PCAC and the Goldberger-Trieman relation, we can use

$h_A(q^2) \simeq \frac{2M g_A(\mu^2)}{\mu^2 - q^2}$  when  $q^2 \simeq \mu^2$ . By doing this, we see that the coefficient of  $q^\mu$  vanishes when  $q^2 \simeq \mu^2$ . So with  $q^2$  in this region,

$$\langle p_2 | A^\mu(0) | p_1 \rangle \simeq \bar{U}(p_2) g_A(q^2) \gamma^\mu \gamma_5 U(p_1).$$

7. We have made some changes from the definitions in Bincer's paper (Ref. 1). The most notable change is a change of variables from Bincers  $W$  to  $W^2$ . A complete discussion of this change and the resulting change in the definitions of the off-shell form factors is unnecessary for our purposes. For a detailed discussion see D. J. Silverman, Ph. D. dissertation, Stanford University Physics Department, Stanford, California, (1968) (unpublished).
8. To examine the  $q_1 \rightarrow 0$  limit, we use an analysis similar to that used by S. L. Adler to derive strong interaction consistency conditions. See S. L. Adler, Phys. Rev. 139, 1638 (1965).
9. Although the vector form factor does not have a singularity in  $\mu^2$ , its derivative may be singular depending on the model assumed. However, no model gives more than a  $\frac{1}{2}$  for the derivative of the form factor. So the terms containing  $\frac{1}{\mu^2}$  would still be small compared to the  $\frac{1}{\mu^4}$  singularity in the derivative of the induced pseudo-scalar form factor.
10. That the nucleon radius is infinite when  $\mu$  is equal to zero can also easily be seen using the dispersion relation in the photon momentum.

$$F'(0) = \frac{1}{\pi} \int_{4\mu^2}^{\infty} \frac{\text{ABS } F(q^2) dq^2}{q^4}$$

When  $\mu^2 \rightarrow 0$ , the lower limit on the integral is 0. Near  $q^2 = 0$ , the absorptive part is proportional to the  $\pi$ - $\pi$  scattering phase shift which theoretical evidence indicates is finite. Therefore the integral blows up at the lower limit.

11. See Appendix A.
12. See Appendix B.
13. See Appendix C.
14. S. D. Drell and H. R. Pagels, Phys. Rev. 140, B397 (1965);  
R. G. Parsons, Phys. Rev. 168, 1562 (1968);  
H. R. Pagels, Phys. Rev. 140, B999 (1965);  
D. U. L. Yu and L. Grunbaum, Bull. Am Phys. Soc. 13, 24 (1968).
15. P. Roy, Ph.D. dissertation, Stanford University Physics Department, Stanford, California, (1968) (unpublished).
16. S. D. Drell, and H. R. Pagels, Phys. Rev. 140, B397 (1965).
17. H. P. Stapp, Report No. UCRL-10261, University of California, Berkeley, California (1962).

TABLE I

GRAPHICAL ELEMENTS FOR THE CURRENTS





$A_{\alpha}^{\mu}(x)$	
$D_{\alpha}(x)$	
$V_{\alpha}^{\mu}(x)$	
$J_{EM}^{\mu}(x)$	

TABLE II

GRAPHICAL ELEMENTS ARISING FROM CURRENT COMMUTATORS

	$i\epsilon_{\alpha_1\alpha_2\alpha_3} V_{\alpha_3}^{\mu_2}(x_2)\delta^4(x_1-x_2)$
	$i\epsilon_{\alpha_1\alpha_2\alpha_3} A_{\alpha_3}^{\mu_2}(x_2)\delta^4(x_1-x_2)$
	$i\epsilon_{\alpha_1\alpha_3\alpha_2} A_{\alpha_3}^{\mu_2}(x_2)\delta^4(x_1-x_2)$

TABLE III

RESONANCES CONTRIBUTING TO THE ABSORPTIVE PART

N'	(1470)	1/2	(1/2 <sup>+</sup> )	P <sub>11</sub>
N	(1550)	1/2	(1/2 <sup>-</sup> )	S <sub>11</sub>
N'	(1710)	1/2	(1/2 <sup>-</sup> )	S <sub>11</sub>
N''	(1750)	1/2	(1/2 <sup>+</sup> )	P <sub>11</sub>

TABLE IV

POWERS OF  $\frac{W^2 - M^2}{M^2}$

INT. STATE	MATRIX ELEMENT	PHASE SPACE	TOTAL
$\pi$ -N	2	1	3
$2\pi$ -N	$\geq 1$	3	$\geq 4$
$3\pi$ -N		5	$\geq 5$

TABLE V

## PROJECTION OPERATOR COEFFICIENTS

$\alpha_1^{2+}$	$M(4W^2  \bar{1} ^2)^{-2} [6l^4 M^2 + \frac{3}{2} l^4 (W^2 - M^2) - \frac{3}{2} l^2 (W^2 - M^2)^2]$
$\alpha_2^{2+}$	$M^3 (4W^2  \bar{1} ^2)^{-2} [4l^4 + 8l^2 M^2 + 4l^2 (W^2 - M^2) - 2(W^2 - M^2)^2]$
$\alpha_3^{2+}$	$(4W^2  \bar{1} ^2)^{-2} (W^2 - M^2) (-3l^2 M^2)$
$\beta_1^{2+}$	$M(4W^2  \bar{1} ^2)^{-2} (W^2 - M^2) [\frac{3}{2} l^4 - 3/2 l^2 (W^2 - M^2)]$
$\beta_2^{2+}$	$M(4W^2  \bar{1} ^2)^{-2} (W^2 - M^2) [3l^2 M^2]$
$\beta_3^{2+}$	$M^2 (4W^2  \bar{1} ^2)^{-2} (W^2 - M^2) [-3(W^2 - M^2)]$

TABLE VI

CONTRIBUTIONS TO THE ABSORPTIVE PART COMING  
FROM THE  $\pi$ -N INTERMEDIATE STATE

$\alpha_1^{2+}$	$-\left(\frac{W^2-M^2}{M^2}\right)\left(\frac{3M^{5,6}}{4W^4 \bar{1} ^4}\right)\left(1 + 1/4\left(\frac{W^2-M^2}{M^2}\right)\right)$
$\alpha_2^{2+}$	$\left(\frac{W^2-M^2}{M^2}\right)^2\left(\frac{M^{5,2}}{2W^4 \bar{1} ^4}\right)(1^2 + 2M^2)(\text{angles})$
$\alpha_3^{2+}$	$-\left(\frac{W^2-M^2}{M^2}\right)^2\left(\frac{3M^{6,4}}{8W^4 \bar{1} ^4}\right)(\text{angles})$
$\beta_1^{2+}$	$\left(\frac{W^2-M^2}{M^2}\right)\left(\frac{3M^{3,6}}{4W^2 \bar{1} ^4}\right)\left(1 - 1/4\left(\frac{W^2-M^2}{M^2}\right)\right)$
$\beta_2^{2+}$	$\left(\frac{W^2-M^2}{M^2}\right)^2\left(\frac{3M^{6,4}}{2W^4 \bar{1} ^4}\right)(\text{angles})$
$\beta_3^{2+}$	$-\left(\frac{W^2-M^2}{M^2}\right)^2\left(\frac{3M^{7,4}}{16W^2 \bar{1} ^4}\right)$



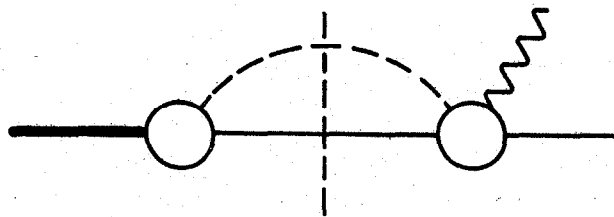


FIG. 1--The  $\pi$ -N intermediate state contribution to the absorptive part.

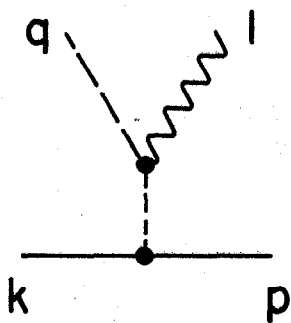


FIG. 2--The pion-pole term of the time-reversed electroproduction amplitude.

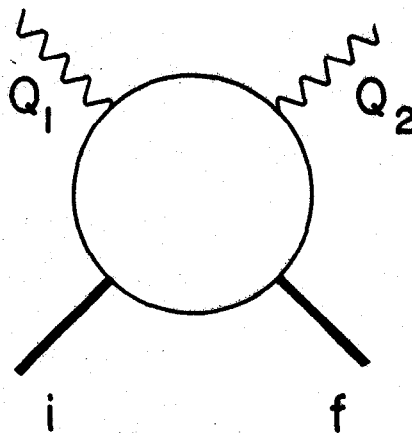


FIG. 3--Graphical representation of Equation (5).

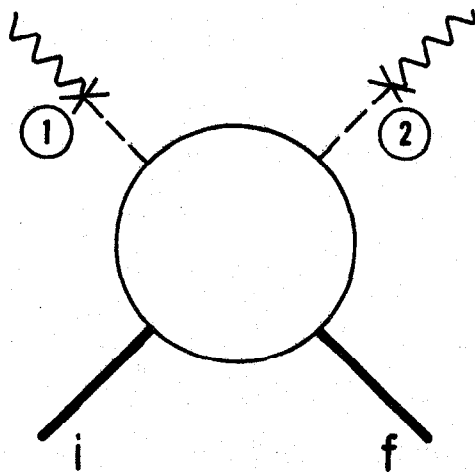


FIG. 4--Graphical representation of Equation (14).

1288A1

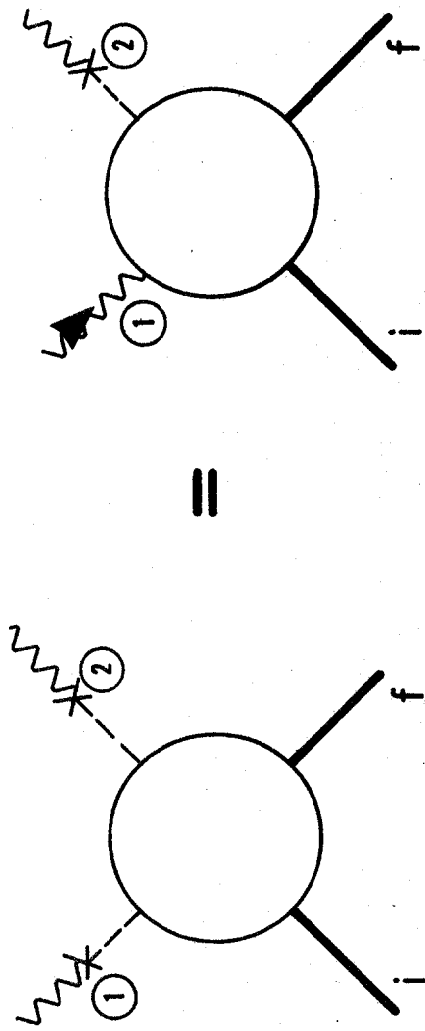


FIG. 5---Graphical representation of Equation (16).

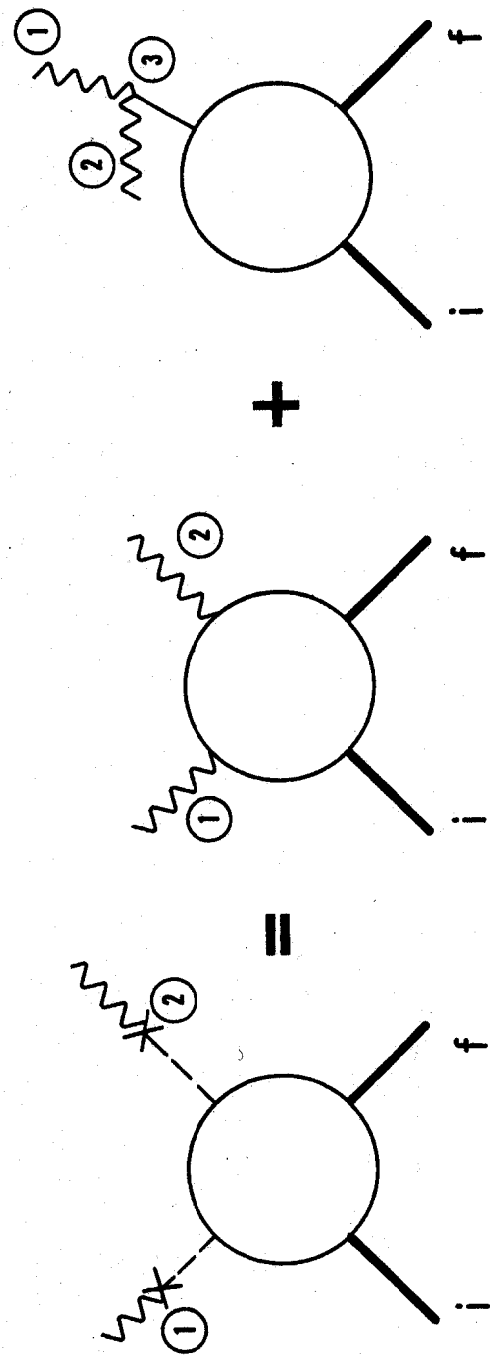


FIG. 6---Graphical representation of Equation (17).

1288A2

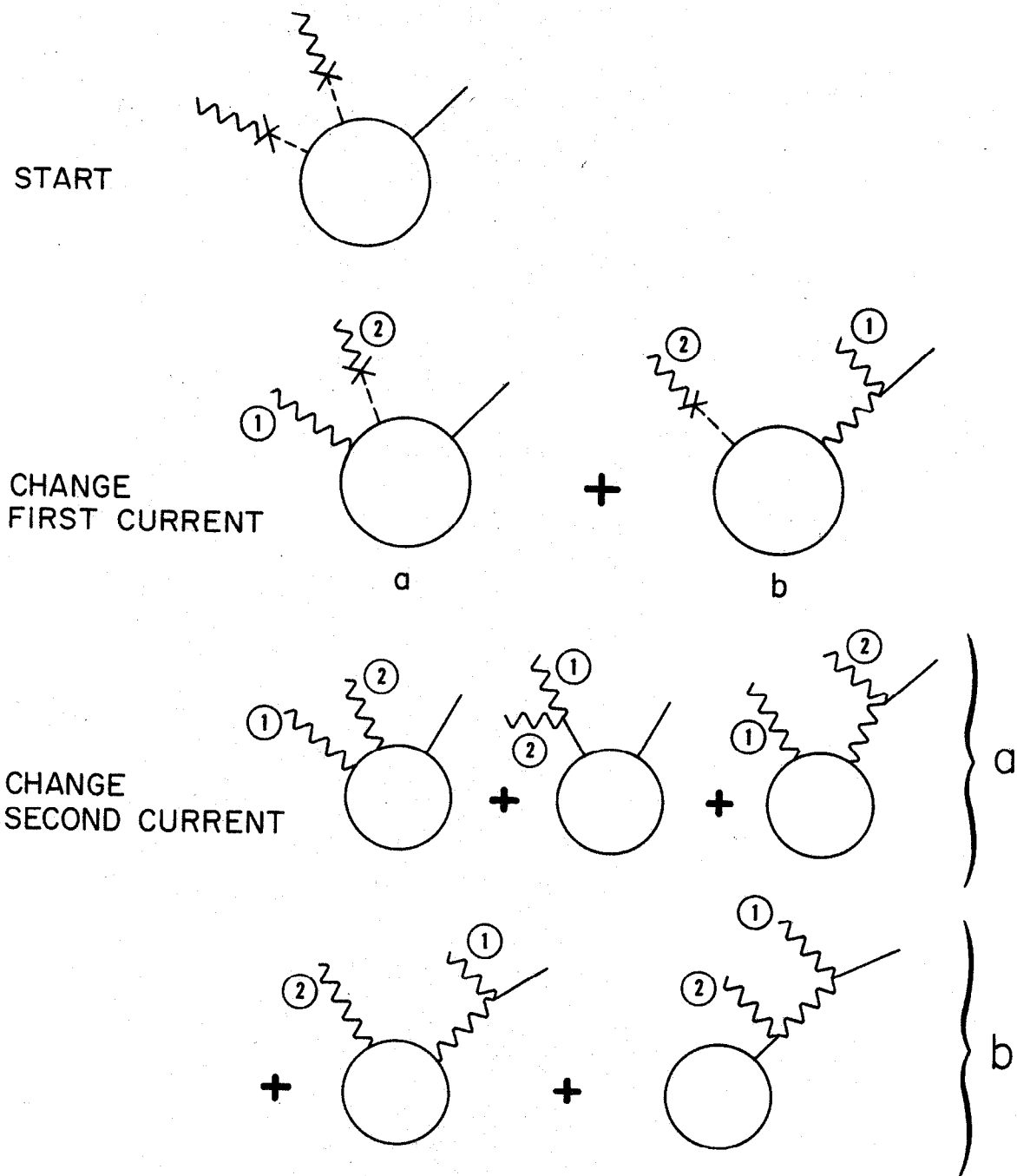


FIG. 7--Graphical reduction corresponding to Equation (18).

1288A3

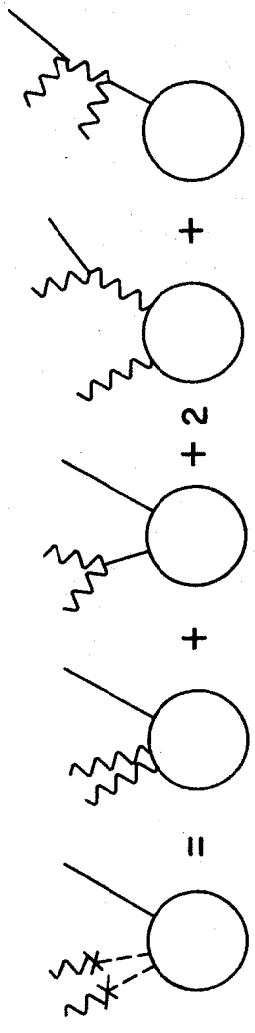


FIG. 8--Simplification of the graphs in Figure 7.

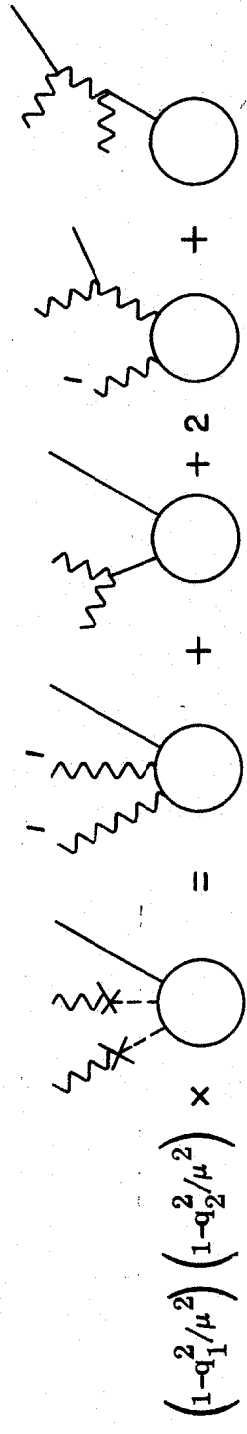


FIG. 9--Representation of Figure 8 after the explicit pion-poles have been removed.

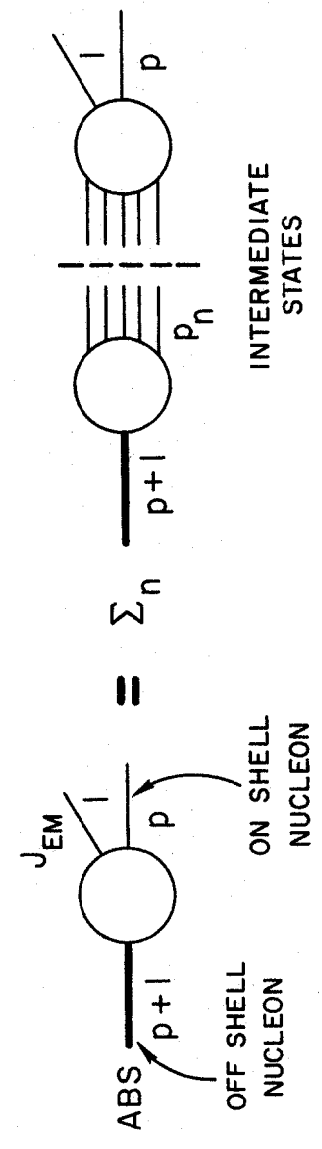


FIG. 10--Graphical representation of the absorptive part.

128884

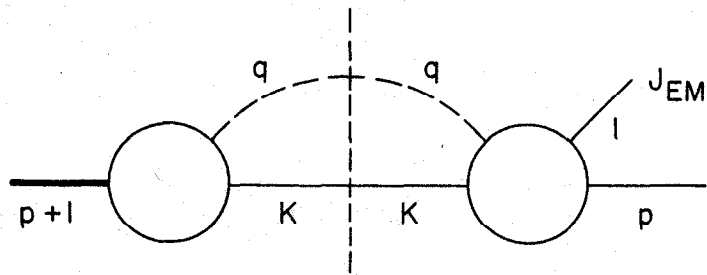


FIG. 11--The  $\pi$ -N intermediate state contribution to the absorptive part.

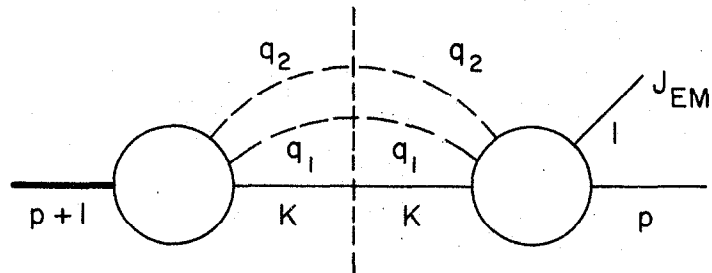


FIG. 12--The  $\pi$ -N intermediate state contribution to the absorptive part.

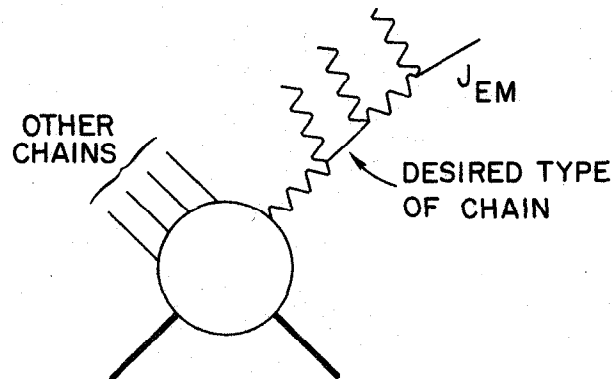
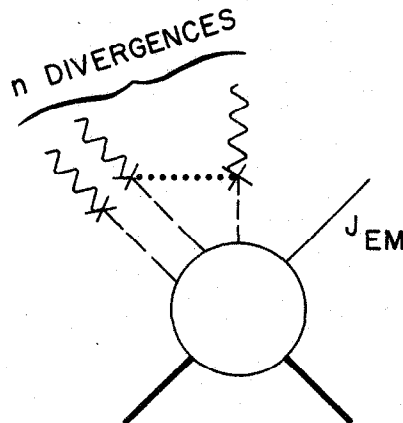


FIG. 13--An example of a dominant graph.



12885

FIG. 14--A typical graph to which the graphical analysis is applied.

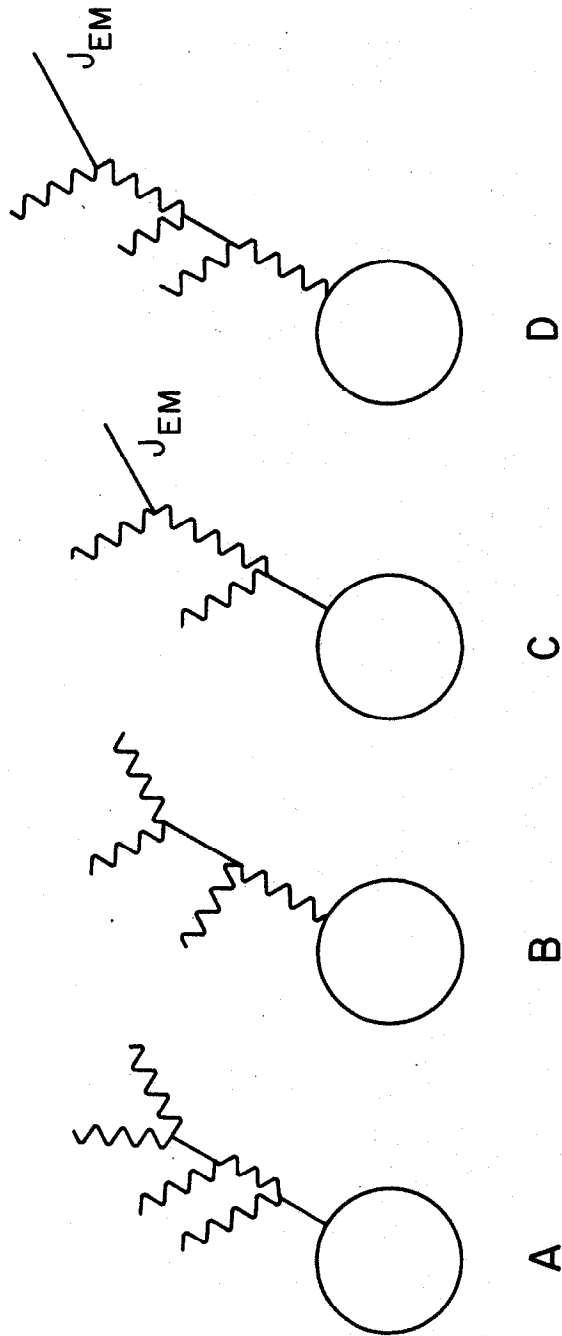


FIG. 15--Examples of the four different types of chains.

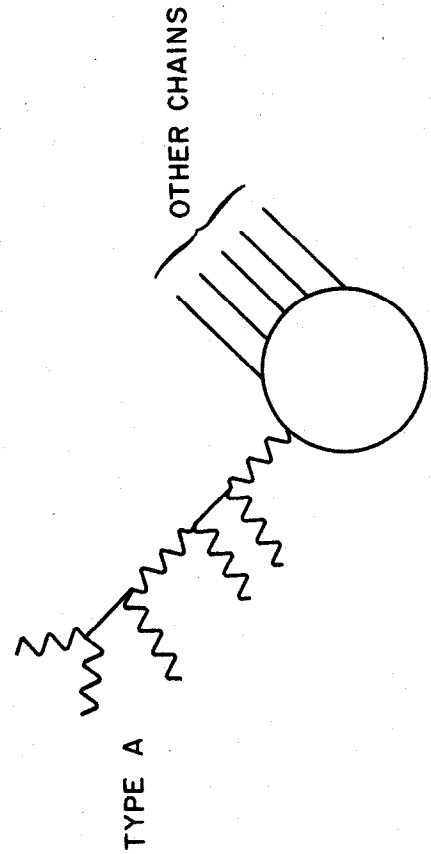


FIG. 16--Graph discussed in the analysis of a chain of type A.

1289A6

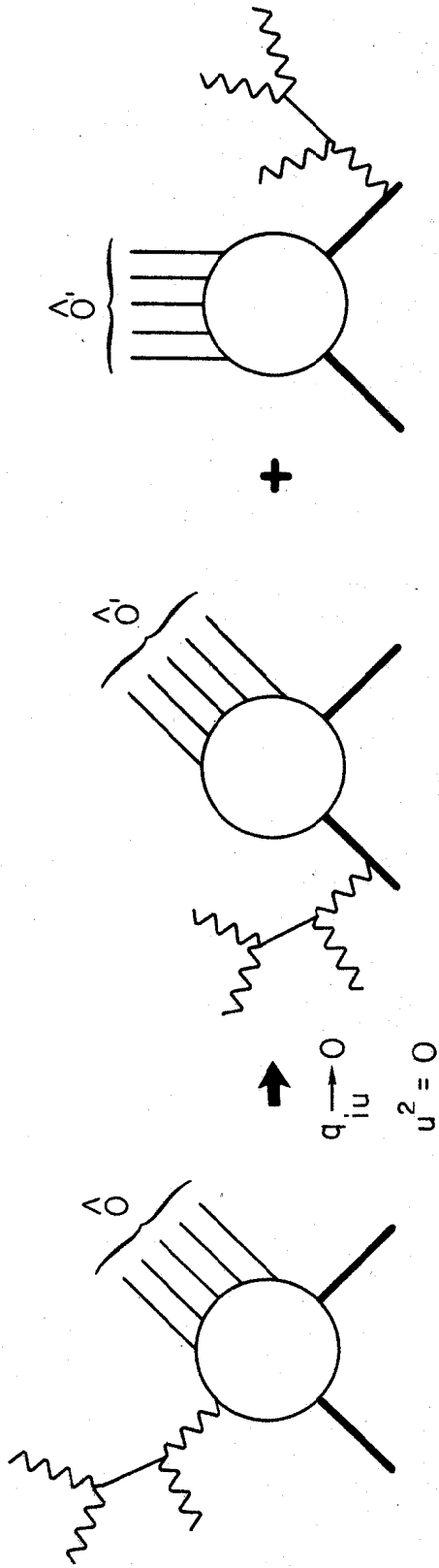


FIG. 17--Symbolic representation of Equation 25.

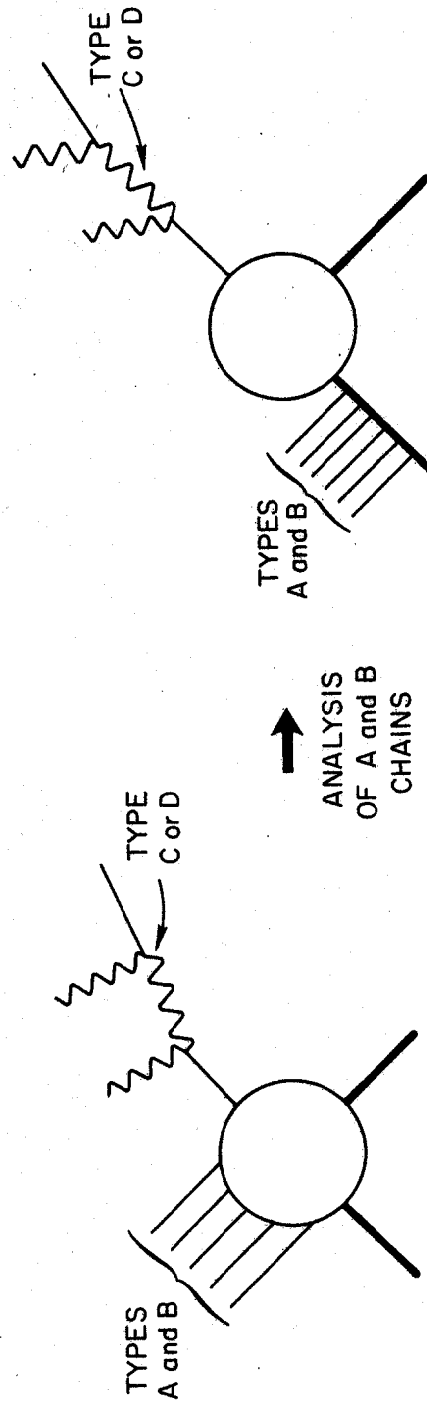


FIG. 18--Symbolic representation of the matrix elements after the analyses of chains of types A and B.

129887

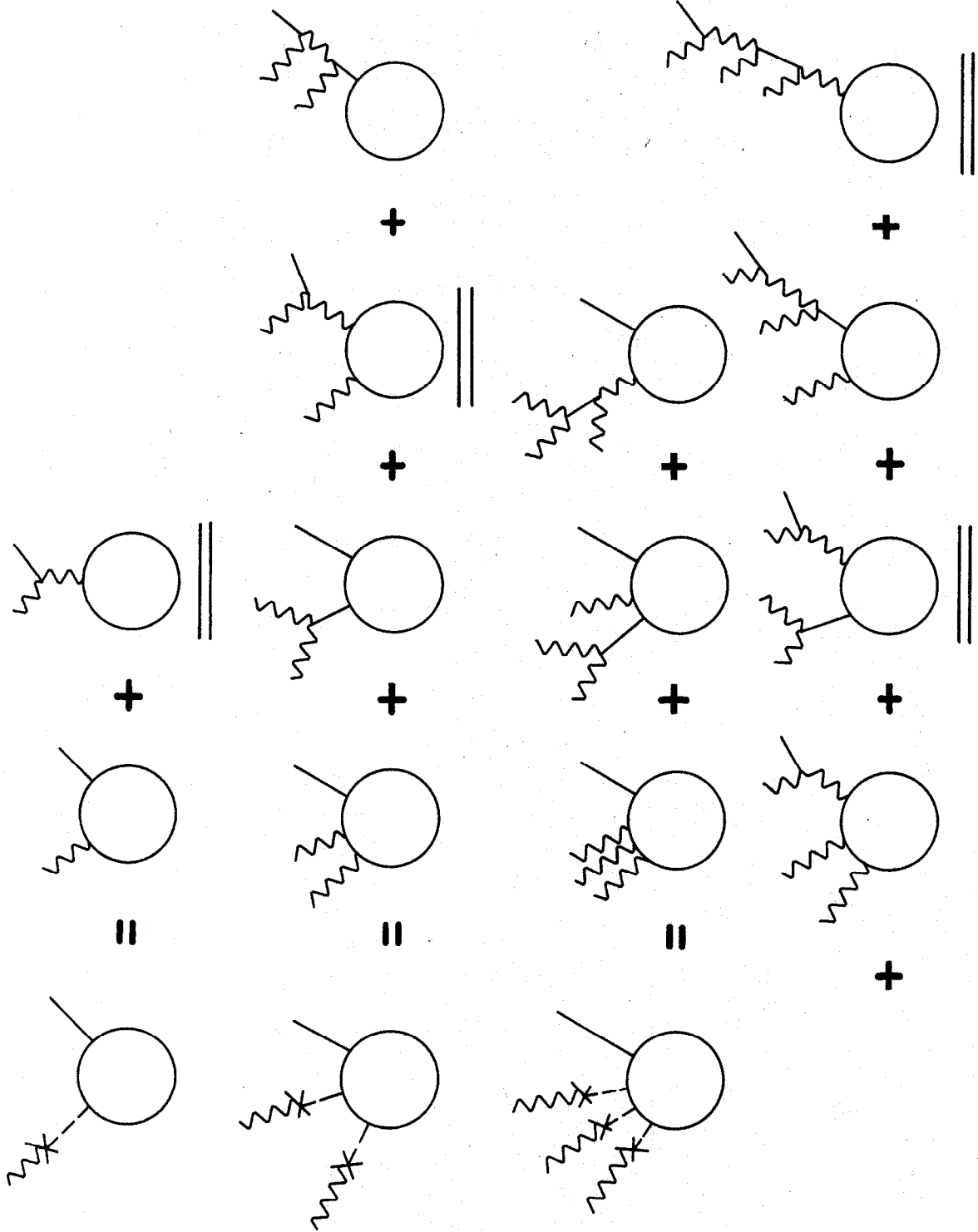


FIG. 19--Graphical expansion of the one, two, and three pion cases.



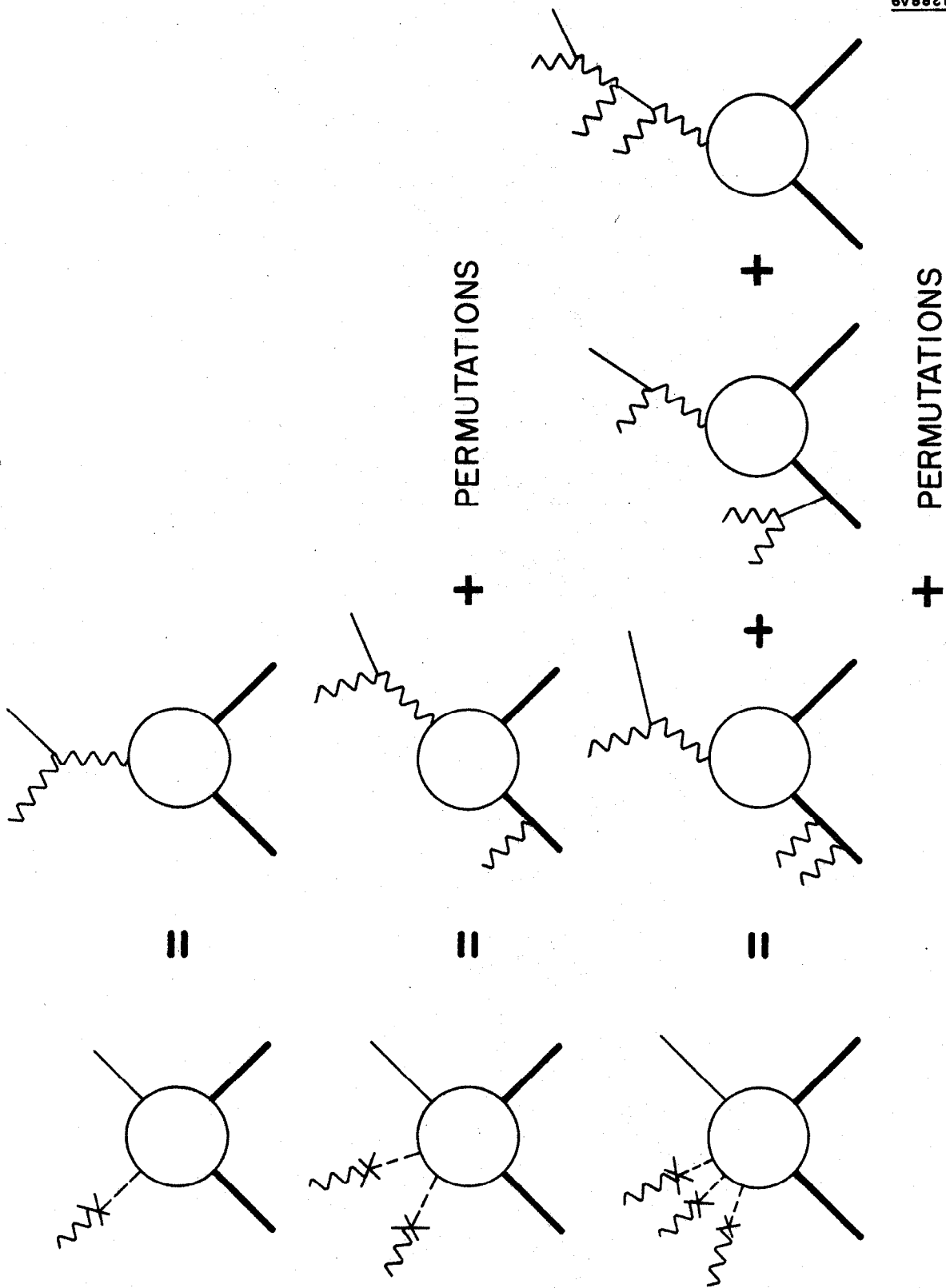
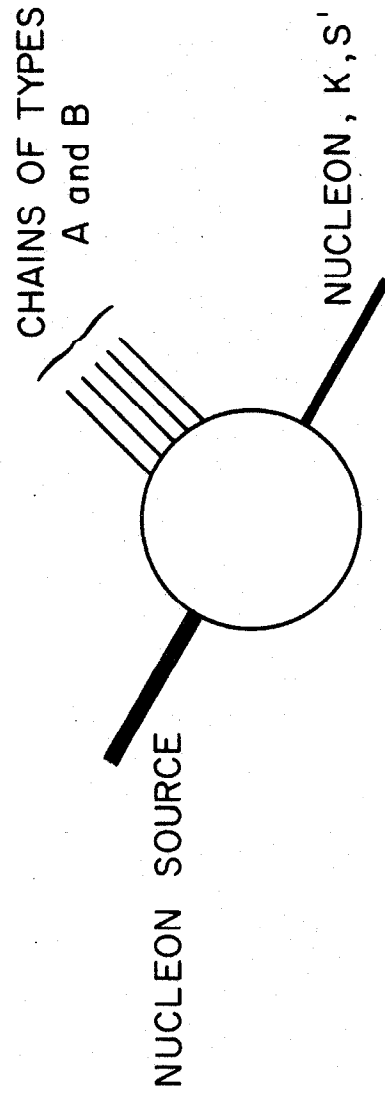


FIG. 20--The dominant graphs in the one, two, and three pion cases in the  $\mu^2 \rightarrow 0$  limit.



1288A10

FIG. 21 -- Typical graph appearing in the analysis of the nucleon source matrix element.